Subpicosecond spectroscopy of hole and exciton self-trapping in alkali-halide crystals

E. D. Thoma, H. M. Yochum, and R. T. Williams*
Department of Physics, Wake Forest University, Winston-Salem, North Carolina 27109
(Received 6 May 1996)

Subpicosecond and picosecond optical absorption spectra following band-gap excitation of alkali-halide crystals have been measured and analyzed. It is found that a simple rule relates the low-energy edge of the ''*N* band'' previously attributed to the one-center (Landau-type) hole polaron, the photon energy of the (two-photon) excitation pulse, and the band gap. This rule describes important features of all subpicosecond absorption spectra of excited alkali halides compiled from the present work and other published works, within the framework of two-photon cross-correlated absorption of the excitation and probe pulses as well as pulse dispersion in the optics and in the sample. It is concluded that the one-center self-trapped hole in alkali halides has not yet been identified by absorption spectroscopy in the visible-uv spectral range. The self-trapped hole and/or associated self-trapped exciton is observed in the two-center configuration. We also report studies using the fourth harmonic of an amplified Ti:sapphire laser to excite insulators with band gaps as large as 11.6 eV by two-photon absorption and observe the subsequent development of defect spectra. [S0163-1829(97)05537-9]

I. INTRODUCTION

Fundamental band-gap excitations of alkali halides, i.e., electron-hole pairs in delocalized band states, are known to localize after a short time to dimensions of the order of a unit cell.[1] Depending on the crystal, 5–10 eV can thus be concentrated in the neighborhood of a few bonds by the existence of this self-trapped exciton,[2] and it is perhaps not surprising that a common outcome is the displacement of lattice ions to form vacancy-interstitial pairs, i.e., *F* centers and *H* centers in the color center terminology.[3] Each stage of this, from the localization of holes and excitons to the appearance of vacancy-interstitial pairs of several distinguishable separations, can be observed by optical absorption spectroscopy conducted on a sufficiently fast time scale.[4–8] The alkali halides are an attractive model system for this kind of study because so much of the background of self-trapping and defect formation has been explored in prior studies. Similar phenomena have been studied in other insulators including silicon dioxide, alkaline earth fluorides, silver chloride, and certain low-dimensional crystals.[2,9]

In the format of time-resolved absorption spectroscopy, the phenomena of self-trapped excitons and defect formation were first studied in the millisecond to 10-ns range with electron pulse excitation;[4,5] then, in the 10-ps range by using two-photon absorption of, e.g., Nd:YAG mode-locked laser fourth harmonic instead of an electron pulse to create electron-hole pairs;[6–8] and more recently subpicosecond studies using laser pulses of a few hundred femtoseconds duration to excite and probe the localized states and defects that result.[9–17] Although important insight was obtained at every major time scale, it is only in the few-ps and sub-ps scale that the processes of self-trapping and the dynamic (i.e., not the slower thermally activated) channels of defect formation can be directly studied.

Iwai and co-workers have made extensive studies of defect formation in the alkali halides in the sub-ps and few-ps time range,[10–17] providing information on the early development of self-trapped excitons, self-trapped holes (V_k centers), and *F* centers in a variety of crystals. A surprising phenomenon that they reported was the *N* band, an absorption feature observed in KI, RbI,[10–14] KBr,[15,16] and NaBr (Ref. 15) at very early time, before the absorption bands of the V_k center (two-center self-trapped hole), self-trapped exciton, or *F* center had developed. The *N* band has characteristically a step like low-energy edge and, at probe delay times of about 1–2 ps, a plateau extending to higher energy above the step. At probe delays $\leqslant 0.8$ ps, the *N* band spectrum in KI and RbI showed structure resolved by Iwai *et al.* into bands named α_1, α_2, and β.[10,11] The low-energy edge of α_1 is the low-energy edge of the whole *N* band. Because the *N* band appeared very early and then disappeared in the same general time as the rise of V_k and self-trapped exciton (STE) bands, and because of reasonable correspondence to transition energies predicted by their embedded cluster model, the α_1 and α_2 components were attributed by Iwai *et al.*[10,11] to the one-center self-trapped hole, i.e., a small polaron involving cubic-symmetry ionic displacements around the hole. The structure of a two-center self-trapped hole (V_k center) in alkali halides is well understood because it survives a long time as a stable defect at low temperature, and can therefore be studied by electron paramagnetic resonance (EPR), optical spectroscopy, polarization analysis, hopping transport, etc.[2] Its stabilization comes mainly from hole-induced formation of a covalent bond between two adjacent halide ions, with subsequent (mainly diatomic) lattice relaxation. This two-center covalently bonded configuration was for a time assumed to be the first, as well as most stable, channel of hole self-trapping in alkali halides. Until the work of Refs. 10–17, there were no optical spectra in the visible-uv range attributed to a one-center, Landau-type[18] self-trapped hole in alkali halides. One-center self-trapped excitons and self-trapped electrons are known in condensed rare gases, for example, but the localization mechanism and configuration in those materials are quite different from the alkali halides.[2] Iwai *et al.*[10,11] calculated transition energies expected for a one-center self-trapped hole in KI, finding reasonable agreement with the energy of the observed *N*

band. By implication, the *N* bands observed in other crystals such as RbI, KBr, and NaBr were suggested also to arise from the one-center self-trapped hole.[10–16]

Iwai and Nakamura observed that the *N* band in KI and RbI is produced for certain values of the (two-photon) excitation photon energies used to excite the crystal, and not by others. They interpreted this in terms of different relaxation pathways out of different electron-hole pair states reached in the two-photon excitation process.[12,13] Furthermore, Shibata *et al.*[17] did not observe an *N* band in KBr when using 4.1-eV photons for two-photon excitation of the crystal, whereas Fujiwara *et al.*[15] found an obvious *N* band in KBr when using 4.62-eV photons for excitation across the 7.4-eV band gap.

We have spent some time reviewing the *N*-band data here, because it is a recently discovered spectroscopic feature which, if correctly interpreted as evidence for initial one-center localization of holes in alkali halides, represents a fairly long-lived ($\sim$1 ps) hole localization step prior to relaxation into the two-center (V_k) configuration. The two-center STH forms the core of the known self-trapped exciton and is important in subsequent defect formation processes. One-center self-trapping of a hole by cubic lattice polarization is dynamically in competition with covalent bond (excimer) formation between the open-shell halogen atom and one of its halide ion neighbors. Because of the large relaxation energy of the excimer, it is the stable configuration. An important question is whether it is preceded by the one-center small polaron for a significant and observable time, and whether the *N* band is its observable manifestation, thereby identifying the time scale as about 1 ps. The data reported in this paper provide information regarding the *N* band and its interpretation. In addition, data, different materials studied, and some refinements of the zero of the time scale growing out of the considerations of ultrafast spectroscopy in fairly thick ($\sim$0.5 mm) dispersive samples such as alkali-halide crystals are presented.

This study was not begun as an investigation of the *N* band, but rather as an extension of ultrafast absorption spectroscopy to wider band gap crystals than studied before, by use of fourth-harmonic Ti:sapphire pulses (5.8 eV) to achieve two-photon excitation across gaps up to 11.6 eV. Data on SrF_2 obtained in this way will be presented in this paper. Because the fourth-harmonic wavelength (214 nm) lies in the highly dispersing region near the fundamental edge of the BaB_2O_4 (BBO) harmonic generating crystals and some of the samples, pulse dispersion considerations have fairly severe consequences for deep-uv excitation and uv-visible probing. Part of what we present here is a description of the use of such pulses in the context of defect spectroscopy in alkali-halide and other insulating solids. In the process of measurements with the fourth harmonic on a familiar sample, KCl, we happened onto the *N*-band phenomenon where it had not been seen before and the study took a somewhat different turn involving third and second harmonics of Ti:sapphire and some smaller-gap halide crystals.

II. EXPERIMENT

A. Overview

A mode-locked Ti:sapphire laser was used to generate 110-fs pulses at a wavelength typically chosen as 855 nm (1.45 eV). Pulses were amplified at 10 Hz in a chirped regenerative Ti:sapphire amplifier with a following linear amplifier stage, which delivered a final pulse energy of up to 5 mJ in a measured pulse duration of 130 fs full width at half maximum (FWHM) at the fundamental wavelength.[19] The amplified fundamental was used to generate the second harmonic (2.91 eV) and either third (4.36 eV) or fourth (5.81 eV) harmonics in β-BaB_2O_4 (BBO) crystals. The harmonics were employed for electron-hole pair generation in the sample through two-photon absorption. BBO is phase matchable for frequency doubling to 205 nm,[20] which implies that two-photon excitation energies up to 12.1 eV are possible. The specifications of the excitation pulses are further outlined in Sec. II B. After harmonic generation, the leftover fundamental beam was separated from the harmonics and passed through an optical delay line which served to provide a variable delay between the excitation and the probe. The fundamental was subsequently focused into a 1.6-mm fused silica plate to generate a white-light continuum which had a usable spectral range from 1.4 to 2.8 eV, limited by detector array response on the low-energy end and by continuum power falloff on the high-energy end. Generally, a single spot on the silica plate could be used for hours at 10 Hz before damage occurred. By using a relatively thin generation medium and by minimizing the thickness of optical components downstream from the generation, dispersion of the frequencies in the continuum prior to sample injection was held to about 8 fs/nm. Using the calculated group velocity dispersion, checked against the experiment at several points through the probe spectrum, chirp-free spectra were interpolated from a dense set of experimental spectra (333-fs intervals in the neighborhood of $t=0$). Convolution effects resulting from non-phase-matched group velocity dispersion of excitation and probe pulses *interacting* in the sample will be discussed and modeled below.

An example of a time series of data for KI before and after correction for white-light dispersion in the optics is shown in Figs. 1(a) and 1(b). Figure 1(a) shows transient absorption as a function of excitation/probe delay in KI after 4.36 eV excitation at $T=50$ K without correction of white-light dispersion. The pulse widths of the excitation and probe were 300 and 140 fs, respectively. It can be seen that the initial absorption appears in the blue region of the optical spectra and then moves down to lower photon energies at later delay times, since the red end of the chirped probe spectrum arrives in coincidence with the excitation pulse when the delay in the probe line is at a later setting than required for coincidence at the blue end. Figure 1(b) displays the same optical absorption after interpolation to correct the 2-ps total chirp has been applied. There is no longer a ''walkover'' of a dispersion-determined edge, but a single step edge which rises at $\sim$1.87 eV, and is in fact the *N* band edge. Although such chirp corrections are widely used in ultrafast studies, it will be seen useful to have reviewed its application in the present context. We will return to the important case of early development of absorption in KI later in this paper.

After continuum generation, collimation, and conditioning by colored glass filters and an aperture, the probe beam was recombined with the excitation beam in a copropagating fashion using a dielectric beam splitter and then focused onto

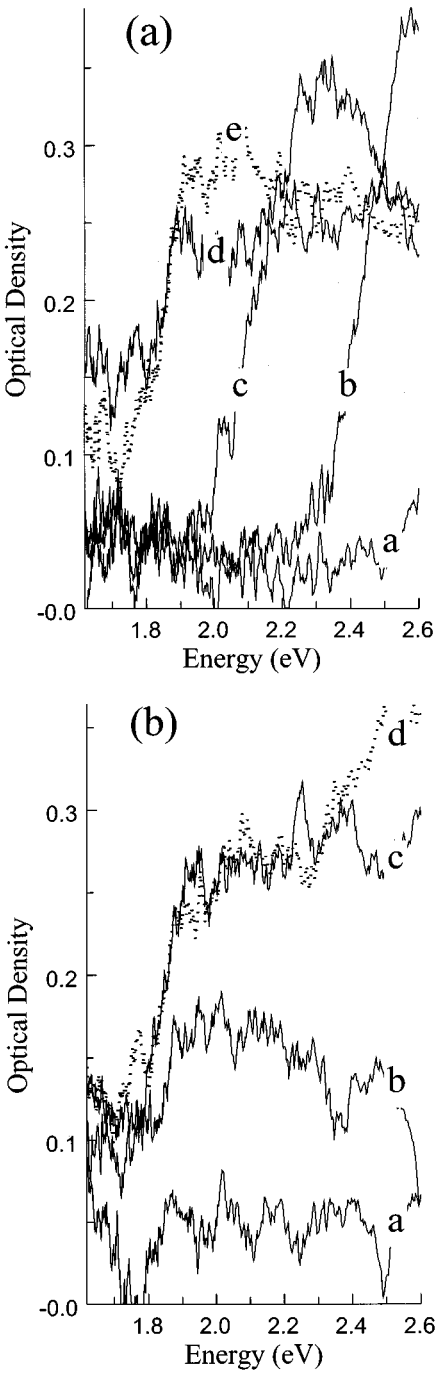

FIG. 1. Transient absorption spectra observed in KI during and after excitation with 4.36-eV, 300-fs pulses at $T=50$ K. (a) presents data which have not been corrected for probe dispersion. Traces $a-e$ represent probe delays which span 2.67 ps at 0.67-ps intervals with the earliest time being a and the latest e. (b) shows data after correction for chirp, where $a-d$ are for probe delays of -0.3, 0.0, 0.3, and 0.7 ps relative to the excitation pulse.

the sample. Although the physical sample thickness was typically 2 or 3 mm in order to get good cleaved surfaces, it will be shown below that the effective thickness of excited and probed regions extends only to a depth of about 500 μm. For low-temperature work, the sample was placed in a closed cycle helium refrigerator positioned by a stepper motor stage such that each laser shot was on a new position on the sample. Prior to recombination of the excitation and probe beams, 4% of the white-light continuum was split off and sent around the sample for use as a reference beam. Measurement of the transmitted and reference spectra was accomplished by a dual channel optical multichannel analyzer and 0.27-m polychromator.[21] A reference probe shot without the excitation pulse and another with the excitation present were taken on each spot before advancing the sample automatically. In this way, 60-shot pairs (typically) were acquired and averaged for each delay line setting. By rastering the sample, approximately 50 such averaged data sets (i.e., approximately 3000 shots) could be acquired before changing the sample. Temporal coincidence between the excitation beam and the probe beam could be determined using frequency mixing in BBO at the sample position. However, because the beams are phase matched in the BBO used for mixing, but not in the cubic sample, we shall show below that a more precise coincidence is obtained from two-photon cross-correlated absorption (TPCCA) in the sample itself. This will be used for interpretation of the data.

The crystals of KI and RbI were grown from zone-refined ultrapure starting material at the University of Utah Crystal Growth Laboratory. Crystals of KCl, KBr, and SrF_2 were grown by Optovac Inc. Although individual impurity analyses of the samples were not made, divalent impurity concentrations in the order of 10^{16} cm^{-3} are typical for these alkali-halide crystals. In the reported experiments, the induced defect optical densities (F center, V_k, or STE) correspond to about 10^{17} defects/cm^3 in the first 0.2 mm, accounting for most of the optical density. This comparison, as well as spectral correspondence to known intrinsic defect bands and the fact that electron trapping by anion vacancies into the F-center ground state is relatively slow, is the basis for our interpretation of the data as representing primarily the interaction of electronic excitations with the intrinsic crystal lattice.

B. Characterization of excitation pulses

The temporal width of the amplified fundamental pulse was measured at 130 fs FWHM using a single-shot autocorrelator.[22] All harmonics derived from the fundamental were generated using type-I phase matching[23] in BBO crystals. The temporal cross-correlation profiles of the harmonics were measured by observing the production of sum (second and third harmonics) or difference (fourth harmonic) frequency generation when mixed with the 130 fs fundamental pulse as a function of optical delay line position. Detection was accomplished by colinear mixing in a 57 °-cut 0.5-mm-thick BBO crystal rotated to the appropriate phase matching angle. Excitation pulse parameters of harmonics produced with BBO crystals of varying thickness used in this work are listed in Table I.

A relatively thick crystal (1.5 mm) was used for generation of the second harmonic since high conversion efficiency could be achieved without undue pulse broadening at this wavelength. The same cannot be said for fourth-harmonic generation. Substantial broadening results from temporal (axial) walkoff of the generating second-harmonic pulse and the produced fourth-harmonic pulse due to significant group velocity differences at the respective wavelengths. An attempt was made to compress the fourth-harmonic pulse us-

TABLE I. Characteristics of excitation pulses used in this work.

BBO crystal thickness (mm)	Generated harmonic	Photon energy (eV)	Pulse energy (μJ)	Pulse width (fs)
1.5	second	2.91	300	190
0.5	third	4.36	5–8	260
0.75	third	4.36	10	300
3.2	third	4.36	20	680
0.5	fourth	5.81	3–6	600
4.0	fourth	5.81	15–20	3500

ing prism pairs with negative net group velocity dispersion (GVD) after the design of Fork *et al.*[24] This compression technique afforded little improvement in the width of the generated fourth-harmonic pulse because most of the stretching was due to the walkoff effect mentioned above rather than simple chirp.

III. RESULTS AND DISCUSSION

Figure 2 shows the development of F-center absorption in KCl at room temperature following two different pump pulses used to create electron-hole pairs by two-photon excitation across the band gap: (a) 5.81 eV, fourth harmonic of Ti:sapphire (3.5 ps, ~ 5 mJ/cm^2); (b) 4.36 eV, third harmonic of Ti:sapphire (0.68 ps, ~ 5 mJ/cm^2). In all other respects, the measurements should be identical. Indeed the F-center spectra in (a) and (b) develop in a very similar way. However, with the 5.81-eV initiating pulse, we observe an ultraviolet absorption band with its low-energy edge around 2.6 eV, which reaches its peak at excitation/probe coincidence ($t=0$) before the F band has developed, and decays thereafter. This appears to be a new band, not seen before in KCl. To give it a short name, we will call it for the time being the manifestation of the N band in KCl. The absorption spectra in KCl measured by Tanimura and Fujiwara[16] with 4.5-eV third-harmonic pulses did not exhibit this N band. Nor did we observe this N band when using 4.36-eV third harmonic pulses to create the electron-hole pairs in KCl, as shown in Fig. 2(b). In that case, the F band simply grows within about 3 ps, without any preceding absorption band in the uv part of the spectrum. The turndown at 2.75 eV is an artifact of second-harmonic contamination in the probe beam.

Figures 3 and 4 present chirp-corrected data showing the development of self-trapped exciton absorption in KI and V_k center absorption in KI:T1, respectively. Both were measured at 47 K as a function of time after e-h pair creation by a 680-fs, 4.36-eV third harmonic excitation pulse. The late spectra ($t \leqslant 11.7$ ps) are similar in both cases, consisting mainly of the 1.7-eV peak due to the σ_u-π_g transition of the two-center self-trapped hole, which is the core of the STE observed in KI and is the V_k center observed in KI:Tl. The ultraviolet absorption around 2.5–2.7 eV is higher for the KI:Tl sample as it rises up toward the main σ band of the V_k center. It also appears accentuated a bit because the spectrometer was tuned farther toward the ultraviolet when studying KI:Tl than when studying KI. The spectra of KI and KI:Tl at early time are very similar to each other, consisting

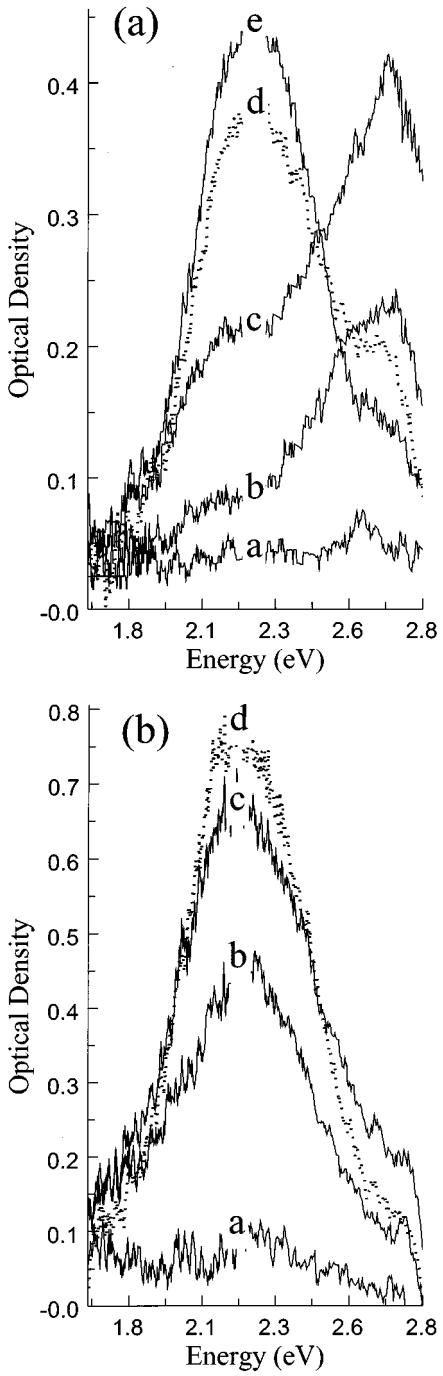

FIG. 2. Absorption observed in KCl under (a) 5.81 eV and (b) 4.36 eV excitation at $T=295$ K. The data have been corrected for chirp, as discussed in the text. The spectra of (a) were acquired for probe delays relative to the 5.81-eV excitation pulse of -6.7, -3.3, 0.0, 6.7, and 13.4 ps, labeled a–e, respectively. The spectra of (b) were acquired for probe delays relative to the 4.36-eV excitation pulse of -0.8, 0.8, 2.5, and 9.2 ps, labeled a–d respectively.

of a step edge at about 1.87 eV (half-height) with lower absorption below this energy, and a broad plateau of absorption above it. The early part of the KI data in this figure duplicates very closely the more recent data set with 300-fs excitation, which were shown in Fig. 1(b). The absorption for $t<2.5$ ps is recognizable by its characteristic step shape and early appearance as the N band reported in KI and KI:NO_2 by Iwai *et al.*[10–14] However, the photon energy at

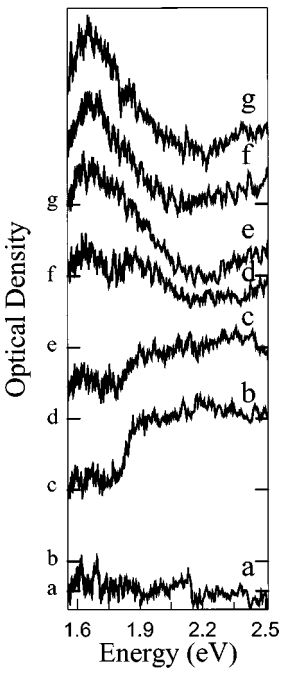

FIG. 3. TPCCA (N-band) and defect absorption in KI measured during and following 4.36-eV, 680-fs excitation at $T=50$ K. The spectra are displayed after chirp correction, for probe delays of -1.7, 0.0, 2.5, 5.0, 11.7, 65.1, and 98.4 ps relative to the excitation pulse, labeled $a-g$ respectively. The zeros of the optical density have been offset 0.12 o.d. between successive spectra except for the first two and are labeled with letters at the left side corresponding to the respective spectra.

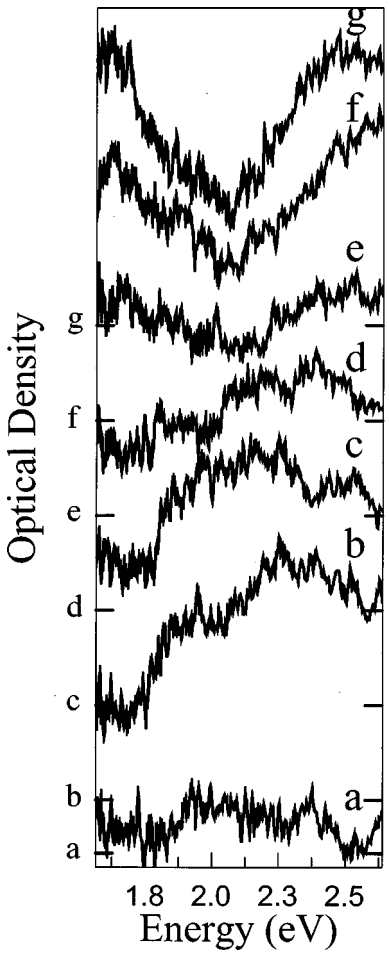

FIG. 4. TPCCA (N-band) and defect absorption in thallium-doped KI measured during and following 4.36-eV, 680-fs excitation at $T=50$ K. The spectra are displayed after chirp correction, for probe delays of -0.2, 0.5, 1.5, 2.5, 3.8, 7.8, and 182 ps relative to the excitation pulse, labeled $a-g$, respectively. The zeros of the optical density have been offset 0.09 o.d. between successive spectra except for the first two and are labeled with letters at the left side corresponding to the respective spectra.

which the step occurs is about 1.87 eV in Figs. 1, 3, and 4, to be compared to ~ 2.17 eV in Ref. 13 and ~ 2.1 eV in Refs. 10 and 11. The energy difference in the N-band step position matches within experimental error the energy difference between the third-harmonic pump pulses used, 4.36 eV in this work and 4.1 eV in Refs. 10, 11, and 13. The N-band step position measured with the continuum probe appears to scale with the photon energy of the excitation pulse.

We also observe an N-band edge in RbI. Figure 5 shows transient absorption in RbI under 4.36-eV, 680-fs excitation, at 333-fs intervals from -0.7 to 1.3 ps. The N-band step is observed at ~ 1.76 eV, to be compared to ~ 2.02 eV in Ref. 12, where 4.1 eV excitation was used. Except for the spectral shift matching the difference in excitation photon energies, the shape of the spectrum is similar to that measured in Ref. 12. The base line ($t<0$ ps) in Fig. 4 slopes downward toward the blue, to negative absorption. This may be due to luminescence contaminating the probe and reference beams in the case of RbI, which was difficult to correct. Luminescence was not a problem in the cases of KI or the other alkali halides we studied.

We observed a similar step edge in KBr under 4.36 eV excitation; however, the step was just at the ultraviolet edge of our observation range, at ~ 2.7 eV. The same type of edge was seen in AgCl and $PbWO_4$ when using second-harmonic Ti:sapphire (2.91 eV) for the excitation pulses. As summarized in Table II, the photon energy of the N-band step edge, $h\nu_{\rm pr}(N)$, always corresponds to the difference between the direct band gap, E_g, and the excitation photon energy, $h\nu_{\rm ex}$, within experimental error. This is true both of our data and the data reported in Refs. 10–17. When the difference of the direct band gap and excitation photon energy falls outside the range of the recorded absorption spectrum, such as in KCl with third-harmonic excitation (4.36 or 4.62 eV),[16] KBr with 3.1 eV excitation,[17] and KI or RbI with 3.1 eV excitation,[12,13] no N band is observed.

The conclusion of Table II can be summarized succinctly in Eq. (1):

$$h\nu_{\rm ex}+h\nu_{\rm pr}(N)=E_g\,. \tag{1}$$

The low-energy edge of the N band coincides with the two-photon cross-correlated absorption edge in every case, i.e., one excitation photon plus one probe photon at the ''N-band edge'' just crosses the band gap. For this and other reasons discussed below, we are confident in identifying the N band observed in our data as the two-photon (cross-correlation) absorption spectrum. We suggest, further, that this is true of all the published N-band observations compiled in Table II.

Two-photon cross-correlated absorption (TPCCA) is a signal which should be expected in this kind of experiment,

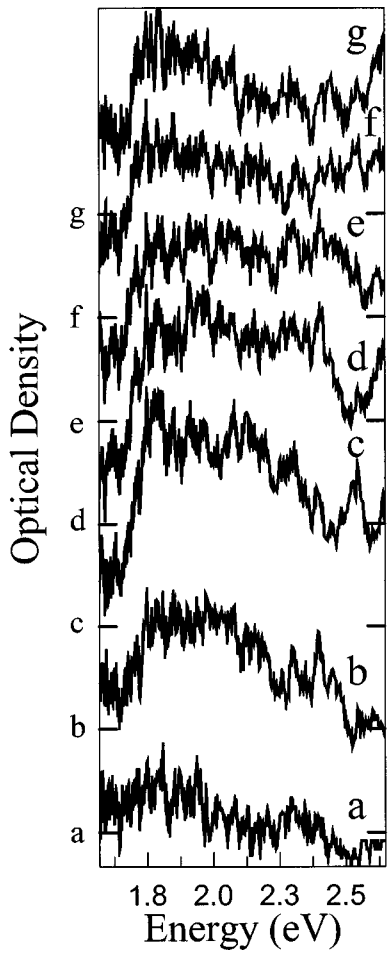

FIG. 5. TPCCA (N-band) and defect absorption in RbI measured during and following 4.36-eV, 680-fs excitation at $T=50$ K. The spectra are displayed after chirp correction, for probe delays of -0.7, -0.3, 0.0, 0.3, 0.7, 1.0, and 1.3 ps, labeled $a-g$, respectively. The zeros of the optical density have been offset 0.12 o.d. between successive spectra and are labeled with letters at the left side corresponding to the respective spectra.

and whose magnitude can be calculated from published two-photon absorption coefficients and the pump beam irradiance. In fact, a simple argument shows that probe attenuation by allowed TPCCA absorption must be comparable to the pump attenuation if the density of allowed final states is comparable. The two-photon attenuation of the probe beam of peak irradiance ($I_{\rm pr}$), where one of the photons is absorbed from the excitation beam of peak irradiance ($I_{\rm ex}$) depends only on $I_{\rm ex}$ (in the limit of nondepleting $I_{\rm ex}\gg I_{\rm pr}$), and on the copropagation length (z) of the excitation and probe beams as stated in the following:

$$I_{\rm pr}(I_{\rm ex},z)=I_{\rm pr}(0)\exp[-\beta z I_{\rm ex}]. \tag{2}$$

The two-photon absorption coefficient $\beta(h\nu_{\rm ex},h\nu_{\rm pr})$ for specific photon energies, and in some cases a two-photon spectrum, are available for several alkali halides.[26–28,31,34,35] The two-photon spectra above threshold are usually rather featureless, and so we have used a representative value of $\beta(h\nu_{\rm ex},h\nu_{\rm pr})$ simply as a constant β in Eq. (2) for the following estimates. Under the simplifying assumption of fixed, nondepleting $I_{\rm ex}$, Eq. (2) just reduces to Beer's law for exponential attenuation of $I_{\rm pr}$, with an effective linear absorption coefficient given by $\alpha=\beta I_{\rm ex}$. In reality, $I_{\rm ex}$ is strongly depleted under conditions of this experiment, according to

$$I(z)=I(0)/[1+\beta z I(0)]. \tag{3}$$

For a typical excitation beam irradiance of $I_{\rm ex}\approx 10^4$ MW/cm^2 and a typical two-photon absorption coefficient $\beta=5\times10^{-3}$ cm/MW, a collimated excitation beam is depleted by two-excitation-photon absorption to $\frac{1}{2}$ value in 200 μm. Based on the fact that we were focusing into the sample and upon our observation of defect track lengths in the sample, an effectively excited depth of roughly 500 μm seems typical, and we adopt this for the analyses to follow. At the same excitation irradiance, we see that an effective ''Beer's law''probe attenuation of $\alpha\approx 50$ cm^{-1} is to be expected at the front of the crystal, and the effective ''linear α'' for the probe decreases from front to back as $I_{\rm ex}$ is depleted. Finally, consider a thin sample so that $I_{\rm ex}$ is nondepleting in any case, and approximate the two-photon spectrum as nearly flat for $h\nu_{\rm pr}+h\nu_{\rm ex}>E_g$. Then it follows that if $\beta(h\nu_{\rm ex},h\nu_{\rm pr})\approx\beta(h\nu_{\rm ex},h\nu_{\rm ex})$, the probe beam attenuation due to allowed two-photon absorption should be comparable to the excitation beam attenuation. Thus TPCCA is a strong effect under typical conditions of this experiment.

The two-photon absorption coefficient depends on the relative polarization of the two beams participating, as shown in the detailed theory of Inoue and Toyozawa[36] and as studied experimentally for alkali halides by Frohlich *et al.*[27,31] For orthogonal linear polarization, the two-photon absorption coefficient is about 67% of its value for parallel polarization in RbI.[27] For KI, RbI, and KBr having the rocksalt structure, the ratio of two-photon absorption coefficients for orthogonal versus parallel polarization falls between 50% and 100%.[31] For CsI and CsBr, having the CsCl structure, the ratio is somewhat below 50% and depends in this case on orientation of the crystal axes with respect to the polarization axes.[31] In the present experiments, the probe and third-harmonic excitation beam had orthogonal polarization while the probe and the fourth-harmonic excitation beam had parallel polarizations. Since the dependence on relative polarization is weak for the rocksalt alkali halides, we have not yet undertaken experiments to vary the polarization.

Equation (1) and the associated discussion so far concerns just the low-energy edge or threshold of the two-photon cross-correlated absorption (TPCCA) signal. Its spectral shape above the edge in raw (dispersive) spectra is determined primarily by which parts of the excitation and probe pulses overlap in the sample for a given delay setting, and also by the two-photon absorption spectrum above threshold. When the part of the probe chirp that results from dispersion in the optics has been corrected by the interpolation method discussed earlier, the spectrum for coincidence of excitation and probe begins to resemble the actual two-photon absorption spectrum. However, there are still differences because relative dispersion of the interacting pulses in the alkali-halide sample produces an additional chirp (which can be large, e.g., in KI) and an axial walkoff effect that is more difficult to extract. To illustrate how apparent spectral shapes as well as persistence times can be influenced when a broad absorption band is measured in a dispersive sample with

TABLE II. Compilation of data on N-band steps observed in subpicosecond spectroscopy of alkali halides and two other materials under two-photon band-gap excitation and continuum probe observation. The probe photon energy at which the low-energy step edge of the N band is observed (at half maximum height) is listed as $h\nu_{pr}(N)$. The photon energy of the excitation pulse which is employed in the experiments to generate electron-hole pairs or excitons by two-photon absorption is listed as $h\nu_{ex}$. Their sum $h\nu_{pr}(N) + h\nu_{ex}$ is listed in the sixth column. The band gap (or two-photon threshold, if available) is listed as $E_g(2h\nu)$ in the last column. In the reference (Ref.) column, the notation ''PW'' refers to the present work. In column 4, the notation ''None$\leqslant x.x$'' indicates that no N-band step edge was observed within the probed spectral range less than $x.x$ eV.

Crystal	Temp. (K)	Ref.	$h\nu_{pr}(N)$ (eV)	$h\nu_{ex}$ (eV)	$h\nu_{pr}(N)+h\nu_{ex}$ (eV)	$E_g[2h\nu]$ (eV)
KI	4	13	2.18	4.1	6.28	6.25[a]
KI	4	13	None$\leqslant$2.6	3.1	$>$5.7	6.25[a]
KI:NO_2^-	80	10, 11	2.10	4.11	6.21	6.20[a]
KI	47	PW	1.87	4.36	6.23	6.23[a]
KI:Tl	47	PW	1.87	4.36	6.23	6.23[a]
RbI	80	12	2.05	4.11	6.16	6.15[b]
RbI	80	12	None$\leqslant$2.6	3.18–3.25	$>$5.85	6.15[b]
RbI	50	PW	1.76	4.36	6.12	6.15[b]
KCl	6	16	None$\leqslant$2.7	4.63	$>$7.33	8.5[c]
KCl	44	PW	None$\leqslant$2.5	4.36	$>$6.86	8.5[c]
KCl	295	PW	None$\leqslant$2.8	4.36	$>$7.16	8.4[d]
KCl	150	PW	$\sim$2.6	5.81	8.41	8.5[c]
KCl	295	PW	$\sim$2.5	5.81	8.31	8.4[d]
KBr	80	16	2.75	4.63	7.38	$\sim$7.4[b]
KBr:NO_2^-	80	15, 16	2.75	4.63	7.38	$\sim$7.4[b]
KBr	80	17	None$\leqslant$3.0	4.11	$>$7.11	$\sim$7.4[b]
KBr	295	PW	$\sim$2.7	4.36	$\sim$7.05	7.2[d]
KBr[e]	295	25	abs.$>$1.6	5.81	$<$7.41	7.2[d]
NaCl	48	PW	None$\leqslant$2.8	4.36	$>$7.16	8.75[f]
NaCl	295	PW	$\sim$2.5	5.81	8.31	8.5[d]
NaBr:NO_2^-	80	15	$\sim$2.4	4.63	7.03	7.1[f]
CsI	50	PW	$\sim$1.8	4.36	6.16	$\sim$6.2[g]
CsBr	48	PW	None$\leqslant$2.3	4.36	$>$6.66	$\sim$7.3[g]
AgCl	295	PW	1.8	2.91	4.71	$\sim$4.9[h]
$PbWO_4$	295	PW	1.9	2.91	4.81	$\sim$5[i]

[a]Reference 26.
[b]Reference 27.
[c]Reference 28.
[d]Reference 29.
[e]Reference 30.
[f]Reference 2.
[g]Reference 31.
[h]Reference 32.
[i]Reference 33.

chirped pulses, we have modeled the spectrum of an assumed flat absorption above the two-photon threshold in KI, as it would be measured by a continuum pulse with dispersion of the silica optics and KI sample taken into account. The simulation also includes the effect illustrated by the following example: For one delay line setting, a certain red wavelength in the probe pulse may overlap the excitation at the front surface of the sample. For a larger delay, the same red-wavelength probe will ''catch up'' to the excitation pulse deeper within the sample—for example, at the back edge of the effective penetration range of the excitation into the sample, estimated as $\sim$500 μm. Thus an instantaneous absorption which is present only during the coincidence of the excitation pulse and this red part of the probe would be observed to persist for a time equal to the transit-time difference of the excitation and the red probe passing through the effective sample thickness. The simulated ''raw'' data such as would be measured in the experiment are shown in Fig. 6(a). That is, Fig. 6(a) has chirp due to the silica optics and KI sample built into it, as well as the summation over delayed coincidence deeper in the sample discussed above. Except for the simplistic flat two-photon spectrum above a sharply sloping threshold which was assumed for simplicity, the simulated ''data'' for KI in Fig. 6(a) should be directly

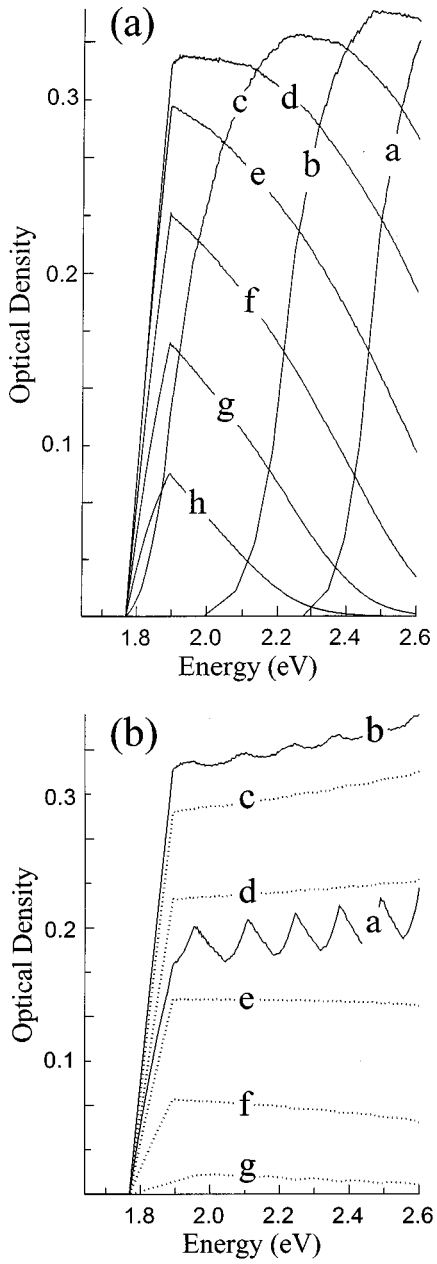

FIG. 6. Simulated TPCCA spectra in KI under 4.36-eV excitation, assuming 500 fs cross correlation of excitation and probe in the sample, a 0.5-mm extinction depth of the excitation pulse, and a flat two-photon absorption spectrum above a 1.87-eV threshold, falling to half-height at 1.83 eV. Part (a) shows simulated chirped spectra as they would be measured, with delays of 0.7 ps between each spectrum, where spectrum *a* is the earliest shown. Part (b) shows the simulated data after the same interpolation correction for chirp that was applied to real data, where probe delays of -0.3, 0.3, 1.0, 1.7, 2.3, 3.0, and 3.7 ps are shown as $a-g$, respectively.

comparable to the real data for KI in Fig. 1(a), conducted with the corresponding pulse durations. The ''walkover'' of the initial rise of TPCCA detected first in the blue end is obvious in both Figs. 1(a) and 6(a). The ''pileup'' at the stationary *N*-band edge corresponding to the minimum-energy two-photon transition is also evident. It can also be seen in both experiment and simulation that the height of the TPCCA signal decreases as it walks over from blue to red.

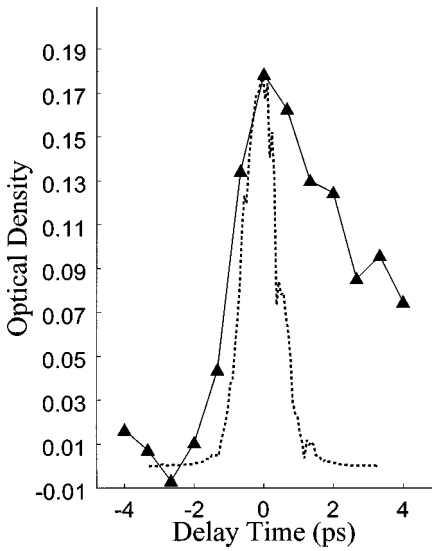

FIG. 7. Dashed curve is the cross correlation of the fourth-harmonic and fundamental pulses measured by difference-frequency mixing in BBO. These pulses were then used, respectively, to excite KCl and to generate the continuum probe used in measuring *N*-band absorption at 2.6 eV. The solid curve (with triangles) is the measured rise and fall of the *N*-band absorption in KCl.

This is an expression of the fact that the blue end of the probe has better group velocity match to the ultraviolet excitation pulse, and therefore experiences longer overlap during transit through the sample.

Next, compare the same real and simulated KI data after correction for chirp in the optics, shown in Figs. 1(b) and 6(b). (The sawtooth superimposed on curve *a* of both figures is an artifact of the chirp-correcting interpolation program which occurred only for early traces.) The important point to notice is that after chirp correction, the two-photon absorption spectrum, with its edge at about 1.87 eV in the real KI data and 1.83 eV in the simulation (the difference being in assumed edge shape), simply rises up and decays in correspondence to overlap of the excitation pulse and the (now chirp-free) probe spectrum. In the real KI data of Fig. 1(b), this is the *N* band. The real data and the simulation differ in the region below the *N*-band edge, because there is STE or defect absorption rising up under the *N*-band edge even as the *N* band decays, in the measured data of Fig. 1(b).

Figure 7 compares the duration of the *N*-band absorption at 450 nm in KCl with the cross correlation (in BBO) of the 214-nm excitation pulse and the 855-nm fundamental pulse, whose duration approximates that of the continuum it generates. For this experiment, the 214-nm light was generated in a 0.5-mm BBO crystal and had the cross-correlation width of $\sim$900 fs (where $\sim$half of the apparent broadening is due to GVD in the difference-frequency mixing crystal used for the measurement). In comparison, the observed duration of the 450-nm TPCCA signal in KCl (solid line) is seen to last much longer than the cross correlation of the same pulses in BBO (dashed line). This is because in difference-frequency mixing for pulse correlation, the requirement for phase matching assures a reduction of group velocity differences, whereas in the cubic alkali halide sample, no phase matching is possible. The observed TPCCA signal will persist for all

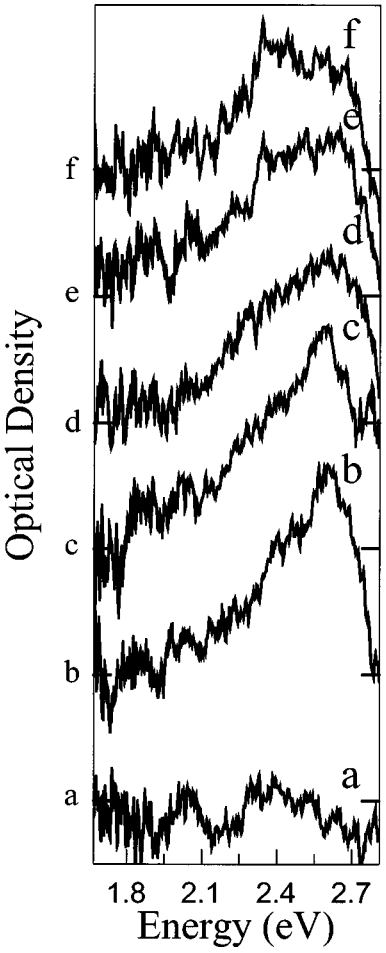

FIG. 8. Transient absorption in SrF_2 under 5.81-eV excitation at $T=295$ K. Probe delays are -1.2, 0.5, 5.5, 13.8, 27.2, and 43.8 ps, labeled $a-g$, respectively. The zeros of the optical density have been offset 0.1 o.d. between successive spectra and are labeled with letters at the left side corresponding to the respective spectra.

delay settings for which the probe photon $h\nu_{pr}(N)$ can overtake the slower-moving excitation pulse at some depth within the sample.

In KI, this effect is more severe because dispersion is steeper in the measurement and excitation range. The width of the convolution of overlaps of a 1.87-eV probe and a 4.36-eV excitation pulse propagating *in only a 500-μm thickness of KI* amounts to ~ 2.2 ps, comparable to the simulated result in Fig. 6. This prediction is obtained straightforwardly from calculated group velocities, but we also confirmed it by direct measurement of the propagation time for pulses at different wavelengths through a piece of KI. The transit-time difference for 855-nm and 285-nm pulses traversing a 1-mm thickness of KI is 3.3 ps, as directly measured.

Having stated that this project was undertaken at first in order to study wide-gap insulators such as alkaline earth fluorides with Ti:sapphire fourth-harmonic excitation, we present in Fig. 8 the spectra of absorption in SrF_2 following band gap excitation at room temperature. The absorption of two 5.8-eV photons can supply 11.6 eV, whereas the band gap of SrF_2 is 11.4 eV. Thus, the excitation pulse populates states about 0.2 eV above the band gap. The induced absorption spectrum is observed to achieve full strength within about 500 fs after coincidence of excitation and probe pulses, and it does not grow significantly during the following 43 ps. The fourth-harmonic pulse width in this experiment was 3.5 ps, and the probe pulse width was ~ 140 fs. The shape of the spectrum is similar to the bound-electron transitions of the STE in SrF_2.[2,37] The hole transitions of the STE in SrF_2 lie outside the spectral range of the present measurement. We are observing very rapid (<500 fs) rise of bound electron transitions in SrF_2 after excitation of electron-hole pairs of energy slightly in excess of the band edge.

The most straightforward interpretation is that the electron-hole pairs relax into self-trapped excitons in less than 500 fs. Such an *e-h* pair self-trapping time is more similar to the STE formation time in SiO_2 (150 fs) (Ref. 9) than to the slower STE formation time (5–10 ps) observed in alkali halides such as KCl, KI, and RbI in Refs. 10–14 and 16 and the present work. Since it is not yet clear why the self-trapping rate of *e-h* pairs is so much faster in SiO_2 than in alkali halides, we cannot say whether the fast rate in SrF_2 is expected. However, since SrF_2 is behaving differently from other halides (i.e., alkali halides), it is worth considering an alternative hypothesis for electron trapping in the pure crystal that may be unique to the alkaline-earth fluorides, as discussed below.

It is known that a bound electron-hole pair relaxes to a self-trapped exciton in the configuration of a nearest-neighbor *F-H* pair in fluorite crystals, i.e., a fluorine vacancy trapping an electron and a fluorine atom in an adjacent interstitial site. As another possibility to account for prompt electron trapping in an excited perfect crystal, we direct attention to a mechanism suggested by Catlow,[38] by which perturbed *F* centers might be generated in fluorite crystals without waiting for electron-hole pairing. Catlow examined whether it is energetically favorable for a conduction electron in fluorite to spontaneously relax to a neighboring pair of an *F* center and interstitial fluoride *ion*, an *F-I* pair. He found that this form of electron self-trapping is theoretically exothermic in CaF_2 and BaF_2, but slightly endothermic in SrF_2. However, it was noted that the small positive energy of the process in SrF_2 is within the range of errors of the calculation, and so this form of self-trapping might proceed exothermically in SrF_2 as well. If this kind of process is occurring, then the appearance of trapped electron states in a crystal which was perfect before excitation does not pre-suppose bimolecular electron-hole pairing from band states,[39] and so the appearance time could be very fast and independent of excitation density. So far, there is no evidence of *F-I* pairs formed spontaneously by conduction electrons. We do not yet know how the bound-electron part of the absorption spectrum of an *F-I* pair should differ from that of an *F-H* pair. To pursue the possibility spectroscopically, one might use shorter fourth-harmonic excitation pulses and study absorption rise time as a function of excitation density.

IV. CONCLUSIONS

The identification of two-photon cross-correlated absorption as the origin of the ''*N* band'' observed in subpicosecond absorption spectroscopy of alkali halides leads to reassessment of at least four prior conclusions or hypotheses drawn from the phenomenon. In particular, the circumstances leading to the observed presence or absence of the *N*

band in a given experiment suggested several hypotheses in the past which, though all physically reasonable, seem now most simply explained by Eq. (1).

(a) Iwai *et al.* noticed that in RbI and KI, when $h\nu_{ex}$ was 4.1 eV they observed the N band, whereas when $h\nu_{ex}$ was 3.04 and 3.1 eV, respectively, the N band was not seen.[12,13] Since the energy of $2(h\nu_{ex})$ substantially exceeds the band gap in the former case, but falls within the $2p$-exciton band below the interband edge in the latter, they hypothesized that energy-dependent branching of the relaxation of holes or excitons was being observed. Accordingly, it was suggested that $2p$ excitons in these crystals relax directly to STE's without formation of a one-center STH or an associated one-center STE, whereas electron-hole pairs created by excitation above E_g result in initial relaxation of the holes to the one-center STH. However, the evidence provided by all the data compiled in Table II and the supporting results discussed in this paper establish two-photon cross-correlated absorption $(h\nu_{ex}+h\nu_{pr})$ as the origin of the N-band step edge. A nearly symmetric band near 2.1 eV was observed in KI for $h\nu_{ex}=3.25$ eV in Ref. 13, suggesting that a real feature may lie beneath the obscuring TPCCA step in some cases. The hypothesis of different branching from $2p$ exciton and free carrier states to a presumed one-center STH is unable to account for the conditions of presence or absence of the N band in KBr and KCl. (See Table II.) Furthermore, as discussed earlier in this paper, a one-center STH hypothesis for the N band fails to account in any case for the observed quantitative scaling of the energy of the N-band edge with $h\nu_{ex}$, which is summarized in Eq. (1) and confirmed in Table II.

(b) The two measurements on KBr reported in Refs. 15 and 17 seem to amount to nearly the same observation we made in KCl upon changing the excitation photon energy. In Ref. 17, with $h\nu_{ex}=4.11$ eV, the probe photon would have to be $h\nu_{pr}=3.29$ eV to satisfy Eq. (1) with the band gap $E_g=7.4$ eV of KBr. This probe requirement was above the 1.4–3.05-eV range of the probe spectra, and no N band was observed in that work. The implied absence of one-center hole self-trapping in KBr was then suggested[14] to be due to the wider valence band of KBr relative to KI and RbI (in which the N band had been seen). However, later measurements by Fujiwara and Tanimura[15] using third-harmonic Ti:sapphire pulses ($h\nu_{ex}=4.63$ eV) showed a strong N-band step in KBr at $h\nu_{pr}=2.75$ eV. As seen in Table II, the step position in KBr at $h\nu_{pr}=2.75$ eV satisfies Eq. (1). Thus, although it can be expected on general grounds that hole self-trapping will occur more readily when the valence band is narrow, the N-band observations of Refs. 14 and 15 do not provide an example of this in regard to one-center hole self-trapping.

(c) Shortly after observing the 2.6-eV ultraviolet absorption band in KCl using $h\nu_{ex}=5.8$ eV, and prior to realizing that it originated from TPCCA (N band), we suggested that it might be part of the spectrum of the V_k-like core of the STE, which could be rendered unobservable when using $h\nu_{ex}=4.36$ eV due to optical bleaching by overlap of the strong excitation pulse with part of the uv STE absorption.[25] However, this hypothesis cannot fit the wide array of data in Table II as can the TPCCA hypothesis, and so we conclude that TPCCA is the proper explanation of the N band in KCl as well as the other alkali halide

(d) Since we believe that the principal features of the N band, particularly the step edge at its ''α_1 component,'' are not ascribable to a one-center self-trapped hole, but rather to the phenomenon of two-photon cross-correlated absorption, we should examine carefully what is implied about the existence or properties of a one-center STH in alkali halides. Electron and hole polarons certainly exist in the alkali halides. A variety of measurements, e.g., pertaining to charge transport and to coupling of optical energy to the lattice, as well as extensive theoretical treatments, are ample proof. What is at issue here is whether a hole polaron self-traps on one lattice site for a time of the order of 1 ps without involving covalent bond formation in the two-center V_k geometry, and whether such a one-center self-trapped hole has optical absorption transitions at about 2.4 and 3.3 eV in KI as predicted by the embedded molecular cluster calculation of Iwai and co-workers.[10,11] Except for the observation with $h\nu_{ex}=3.25$ eV in Ref. 13, there is no spectroscopic evidence for presence of a one-center STH transition around 2.4 eV which could be distinguishable from the TPCCA signal. The predicted 3.3-eV transition would overlap the broad (and perhaps vibrationally hot) V_k band of the two-center STH, and so it will be difficult to unravel growth of absorption of the two-center STH and a presumed overlapping one-center STH, without the lower-energy (2.4 eV) transition as a corroborating guide. A better analysis and dissection of the growth of ultraviolet absorption should be possible if one can generate a quality ultraviolet continuum probe extending over most of the V_k band, i.e., up to $\sim$4.5 eV. Efforts in this direction are underway. But for the time being, we conclude that there is no direct spectroscopic evidence for a one-center STH with transitions in the spectral range of the present study.

ACKNOWLEDGMENTS

This work was supported by NSF Grant No. DMR-9510297. We thank P. Sheldon, M. Leblans, and M. Binkley for experimental assistance, K. Tanimura, A. L. Shluger, A. Nakamura, and N. Itoh for helpful discussions and copies of papers before publication, and F. Luty for KI:Tl and KI:NO_2 samples.

*Author to whom correspondence should be addressed.

[1] M. Ueta, H. Kanzaki, K. Kobayashi, Y. Toyozawa, and E. Hanamura, *Excitonic Processes in Solids*, Springer Series in Solid State Sciences Vol. 60 (Springer-Verlag, Berlin, 1986).

[2] K. S. Song and R. T. Williams, *Self-Trapped Excitons*, Springer Series in Solid State Sciences Vol. 105 (Springer-Verlag, Berlin, 1993).

[3] N. Itoh, Adv. Phys. **31**, 491 (1982).

[4] M. Hirai, Y. Kondo, T. Yoshinari, and M. Ueta, J. Phys. Soc. Jpn. **30**, 1071 (1971).

[5] R. T. Williams and M. N. Kabler, Phys. Rev. B **9**, 1897 (1974).

[6] J. N. Bradford, R. T. Williams, and W. L. Faust, Phys. Rev. Lett. **35**, 300 (1975).

[7] M. Hirai, Y. Suzuki, H. Hattori, T. Ehara, and E. Kitamura, J.

Phys. Soc. Jpn. **56**, 2948 (1987).
[8] J. D'Hertoghe and G. Jacobs, Phys. Status Solidi B **95**, 291 (1979).
[9] S. Guizard, P. Martin, G. Petite, P. D'oliveira, and P. Meynadier, J. Phys.: Condens. Matter **8**, 1281 (1996).
[10] S. Iwai, T. Tokizaki, A. Nakamura, T. Shibata, A. L. Shluger, and N. Itoh, J. Lumin. **60**, 720 (1994).
[11] S. Iwai, T. Tokizaki, A. Nakamura, K. Tanimura, N. Itoh, and A. Shluger, Phys. Rev. Lett. **76**, 1691 (1996).
[12] A. Nakamura, S. Iwai, and N. Moriya, J. Lumin. **72-74**, 835 (1997).
[13] S. Iwai and A. Nakamura, J. Lumin. **66**, 418 (1996).
[14] S. Iwai, A. Nakamura, K. Tanimura, and N. Itoh, Solid State Commun. **96**, 803 (1995).
[15] H. Fujiwara, T. Suzuki, and K. Tanimura, in Proceedings of the 13th International Conference on Defects in Insulating Materials [Mater. Sci. Forum **239-241**, 561 (1997)].
[16] K. Tanimura and H. Fujiwara, in Proceedings of the 13th International Conference on Defects in Insulating Materials [Mater. Sci. Forum **239-241**, 549 (1997)].
[17] T. Shibata, S. Iwai, T. Tokizaki, K. Tanimura, A. Nakamura, and N. Itoh, Phys. Rev. B **49**, 13 255 (1994).
[18] L. Landau, Phys. Z. Sowjetunion **3**, 664 (1932); A. M. Stoneham, J. Chem. Soc. Faraday Trans. 2 **85**, 505 (1989).
[19] Coherent Mira basic model 900-B Ti:sapphire oscillator; positive light TSA-10 Ti:sapphire amplifier.
[20] K. Miyazaki, H. Sakai, and T. Sato, Opt. Lett. **11**, 797 (1986).
[21] Princeton Instruments OSMA (dual 512 array) and Jarrell-Ash Monospec 27 polychromator (150 groove/mm, 450-nm blazed grating).
[22] Positive light model SSA.
[23] R. W. Boyd, *Nonlinear Optics* (Academic, New York, 1992).
[24] R. L. Fork, O. E. Martinez, and J. P. Gordon, Opt. Lett. **9**, 150 (1994).
[25] E. D. Thoma, H. M. Yochum, M. J. Binkley, M. Leblans, and R. T. Williams, in *Proceedings of the 13th International Conference on Defects in Insulating Materials* [Mater. Sci. Forum **239-241**, 565 (1997)].
[26] J. J. Hopfield and J. M. Worlock, Phys. Rev. **137**, A1455 (1965).
[27] D. Frohlich and B. Staginnus, Phys. Rev. Lett. **19**, 496 (1967).
[28] M. Casalboni, C. Cianci, R. Francini, U. M. Grassano, M. Piacentini, and N. Zema, Phys. Rev. B **44**, 6504 (1991).
[29] Two-photon absorption edge at room temperature estimated from low-temperature value.
[30] The low-energy *N*-band edge in KBr under 5.81 eV excitation is below our lowest observation energy, but a prompt and short-lived broad absorption band extending throughout the visible range was observed in that case, and is presumed to be TPCCA above the two-photon edge.
[31] D. Frohlich, B. Staginnus, and Y. Onodera, Phys. Status Solidi **40**, 547 (1970).
[32] *Direct* band edge in AgCl at room temperature estimated from 5.1-eV direct transition onset at 4.2 K (Ref. 2).
[33] V. Kolobanov, J. Becker, M. Runne, A. Schroeder, G. Zimmerer, V. Mikhailin, P. Orkhanov, I. Shpinkov, P. Denes, D. Renker, B. Red'kin, N. Klassen, and S. Shmurak, in *Proceedings of the International Conference on Inorganic Scintillators and Their Applications*, Delft, 1995, edited by P. Dorenbos and C. W. E. van Eijk (Delft University Press, The Netherlands, 1996), p. 249.
[34] *CRC Handbook of Laser Science and Technology* Vol III, *Optical Materials*, edited by Marvin J. Weber (CRC Press, Boca Raton, FL, 1986), pt. 1.
[35] P. Liu, W. L. Smith, H. Lotem, J. H. Bechtel, R. S. Adhav, and N. Bloembergen, Phys. Rev. B **17**, 4620 (1978).
[36] M. Inoue and Y. Toyozawa, J. Phys. Soc. Jpn. **20**, 363 (1965).
[37] R. T. Williams, M. N. Kabler, W. Hayes, and J. P. Stott, Phys. Rev. B **14**, 725 (1976).
[38] C. R. A. Catlow, J. Phys. C **12**, 969 (1979).
[39] R. T. Williams, J. N. Bradford, and W. L. Faust, Phys. Rev. B **18**, 7038 (1978).